Journal of Applied Polymer Science

Effect of OMMTs on Flame Retardancy and Thermal Stability of Poly(ethylene-*co*-vinyl acetate)/LDPE/Magnesium Hydroxide Composites

Mahmood Masoomi, Rouhollah Bagheri, Leila Ahmadkhanbeigi, Mohammad Asgari
Chemical Engineering Department, Polymer Group, Isfahan University of Technology, Isfahan 84156-83111, Iran
Correspondence to: M. Masoomi (E-mail: mmasoomi@cc.iut.ac.ir)

ABSTRACT: The aim of this study was to prepare poly (ethylene-*co*-vinyl acetate) (EVA)/ low density polyethylene (LDPE)/magnesium hydroxide (MH) composites applicable in cable industry with required flame retardancy. For this reason, two types of organo-modified montmorillonites (OMMT) with different surface polarites (Cloisite 15A and Cloisite 30B) at various concentrations, and also combination of these two OMMTs with overall loadings of 2 wt % and 5 wt % were used. The samples were compounded using a twin screw extruder with total (MH + OMMT) feeding of 55 wt % and 60 wt %. Limiting oxygen index (LOI) of the samples containing 2 wt % of OMMTs increased about 16% and dripping was suppressed according to vertical burning test (UL-94V). Thermogravimetric results of EVA/LDPE/MH samples containing OMMT showed that the beginning of second step degradation was shifted about 50°C to higher temperatures. The composite tensile strength results showed enhancement by incorporating some amount of nanoclays with EVA/LDPE/MH composites. Scanning electron microscopy images confirmed that MH particles had better wetting by EVA matrix in presence of nanoclays. Oxidative induction time of the EVA/LDPE/MH/OMMT nanocomposites was 140 min, which was more than that of the samples without OMMT (20 min). Employing the equal weight ratios of the two OMMTs demonstrated a synergistic effect on flame retardancy of the samples according to the both tests results (LOI, UL-94V). X-ray diffraction analysis of the samples confirmed the intercalation/semiexfoliation structure of nanosilicate layers in the bulk of EVA/LDPE matrix. This led to longer elongation at break and thermal stability of Cloisite 15A based nanocomposites. © 2014 Wiley Periodicals, Inc. J. Appl. Polym. Sci. **2014**, *131*, 40452.

KEYWORDS: clay; flame retardance; thermal properties; thermogravimetric analysis (TGA); X-ray

Received 10 August 2013; accepted 16 January 2014
DOI: 10.1002/app.40452

INTRODUCTION

In recent years, fire protection has received a great attention and importance because of various disasters caused by the fire accidents.[1] Among important properties of wire and cable insulation materials, low flammability, and thermal stability are essentially required.[2] The addition of flame retardants is needed to achieve acceptable fire properties required by the standards.[3,4] Low density polyethylene (LDPE) and poly(ethylene-*co*-vinyl acetate) (EVA) and their blends have been widely used in cable industry due to their satisfactory mechanical and physical properties.[3,4] However, the flammability of these materials sparks a drawback that restricts their applications.[4] In recent years inorganic hydroxide fillers have replaced halogen based fire retardants in many applications because of their better environmental compatibility. For example, they have been commonly incorporated with EVA to manufacture halogen-free, and low smoke cables.[5] It is well known that fire retardancy can be achieved by using hydrated mineral fillers such as alumina trihydrate (ATH) or magnesium hydroxide (MH) because of their excellent being nontoxic and smoke-suppressing properties. These compounds act in both the condensed and gas phases. They decompose due to fire heating via an endothermic reaction, and then reduce the temperature of the burning material, and also release water to the produced gaseous phase. Although high filler contents (about 60 wt %) are often required to obtain satisfactory fire retardancy, this will result in a reduction of mechanical and also processing properties of the applied materials.[6] However, one possible way to reduce the needed amount of the filler to reach good fire retardancy is to increase the effectiveness of applied flame-retardant material.[7] Nanoclays have been reported to have positive effects on the flame resistant properties of polyolefins. Their flame retardancy mechanism is related to the char formation while burning, which could slow down the polymer pyrolysis. Employing of the nanosilicate layers in combination with MH is very interesting due to the possible synergistic effects of their fire retardancy.[3,8] The aim of this study was to investigate

© 2014 Wiley Periodicals, Inc.

Table I. Sample Codes and Compositions

Sample	EVA (wt %)	LDPE (wt %)	C15A (wt %)	C30B (wt %)	MH (wt %)
VE	60	40	0	0	0
$V_{-0A2B-53}$	45	0	0	2	53
$V_{-0A2B-0}$	98	0	0	2	0
$VE_{1-2A0B-53}$	27	18	2	0	53
$VE_{1-1A1B-53}$	27	18	1	1	53
$VE_{1-0A2B-53}$	27	18	0	2	53
$VE_{2-0A0B-55}$	27	18	0	0	55
$VE_{2-5A0B-50}$	27	18	5	0	50
$VE_{2-2.5A2.5B-50}$	27	18	2.5	2.5	50
$VE_{2-0A5B-50}$	27	18	0	5	50
$VE_{3-0A0B-60}$	24	16	0	0	60
$VE_{3-5A0B-55}$	24	16	5	0	55
$VE_{3-2.5A2.5B-55}$	24	16	2.5	2.5	55
$VE_{3-2A3B-55}$	24	16	2	3	55
$VE_{3-0A5B-55}$	24	16	0	5	55

V: EVA, E: LDPE, A: C15A, B: C30B.

the effects of two types of organo-modified montmorillonites (OMMT), Cloisite 15A and Cloisite 30B, and the influence of their concentration on the fire retardancy and thermal stability of EVA/LDPE/MH composites, which is an essential property needed in cable industry. Considering the criteria of cable-sheathing, nanocomposites of EVA/LDPE/MH incorporated with the two different clay nanoparticles were manufactured and their flame properties, thermal stability, and also tensile and morphological properties were investigated.

EXPERIMENTAL

Materials

Copolymer of ethylene-vinyl acetate (EVA) containing 18 wt % vinyl acetate with trade name of VS430, (MFI of 2.5 g/10 min at 190°C and 2.160 kg, density of 0.939 g/cm^3, Vicat softening point of 60°C, and tensile strength of 13.7 MPa) was supplied by Seetec Co., South Korea. Low density polyethylene (LDPE), with trade name of LF0200 (MFI of 2 g/10 min at 190°C and 2.160 kg, density of 0.920 g/cm^3, Vicat softening point of 94°C, and tensile strength of 15.7 MPa) was obtained from national petrochemical Co., Tehran, Iran. Magnesium hydroxide (Magnifine H-5 GV) was supplied by Albemarle Co., China. Two organo-modified montmorillonites, Cloisite 15A (C15A) and Cloisite 30B (C30B), with different surface polarities and basal spacing were purchased from Southern Clay Products Inc. The basal spacing for C15A and C30B were reported 31.5°A and 18.5°A, respectively.

Sample Preparation

The nanocomposites were prepared by the following two steps. Firstly, the EVA and LDPE granules, with and without MH and OMMTs, were dry blended in the tumble mixer. Secondly, the mixtures were melt blended in an intermeshing co-rotating twin-screw extruder (Nanjing Co, China) having screw diameter of 21.7 mm and L/D ratio of 40. The temperature profile along the extruder barrel from the feed section to the die section for melt-compounding was 120 to 180°C. The screw speed was 300 RPM. Fifteen nano-composite samples were prepared according to the formulations shown in Table I. VE is representative of EVA/LDPE blend. Each composite series is designated by the first suffix number of VE or V letters. The letter A (or B) is the type of the Cloisite 15A (or Cloisite 30B) and the numbers behind letters A and B represent the weight percentages of C15 A and C30B in the composite samples, respectively. The last two digit number is the weight percentage of MH particles in the composite. The reference samples are designated as: $VE_{1-0A0B-55}$, $VE_{2-0A0B-60}$, VE (0% OMMTs and 55 and 60% MH), $V_{-0A2B-53}$ and $V_{-0A2B-0}$ (the composite without LDPE). Tensile test specimens were obtained using injection molding technique. The test specimens for other tests were prepared using the compression molding at 160°C and 10 bar pressure to obtain 3 and 4 mm thick sheets.

Characterization

Mechanical Properties. Tensile strength and elongation at break were measured by a Zwick Z020 machine with the crosshead speed of 50 mm/min, according to ASTM D638. To perform the tensile test, sheets with the thickness of 3 ± 0.4 mm for each specimen were prepared by means of injection moulding method (holding time of 2 min and melt temperature of 180°C). Then dumbbell-shaped samples were prepared applying a mould cutter (an overall dumbbell length 115 mm, the narrow section width of 6 mm, and the gauge length of 25 mm).

Flame Properties. The flame retardation of the composites was studied by measuring of the limited oxygen index (LOI) and vertical burning test (UL-94V) methods. The LOI values were measured on the specimens with dimensions of 85 × 10 × 4 mm^3, according to the standard oxygen index test ASTM D2863. In this test, the upper part of the specimen is burnt, exposed to a definite amount of oxygen. The oxygen is blown in mixture with the nitrogen in a definite percentage. According to the standard, if the specimen is burnt in more than 3 min, or more than 50 mm the specimen is burnt as other criterion, the oxygen concentration must decrease. Conversely, if the specimen is on fire for less than 3 min, or less than 50 mm of the specimen is burnt, the oxygen concentration must increase. The change in oxygen concentration continues until the specimen is on fire for 3 min, or as other way of measurement, 50 mm of the specimen is burnt for the chosen amount of oxygen. LOI percent is calculated based on eq. (1):

$$\text{LOI}\,\% = \frac{V_{O_2}}{V_{O_2} + V_{N_2}} \times 100 \quad (1)$$

where V_{O_2}, V_{N_2} are volume flow rates of the oxygen and nitrogen, respectively.

The UL-94 vertical test is a test method which was developed for polymeric materials used for parts in devices and appliances. The results are intended to serve as a preliminary indication of their acceptability with respect to flammability for a particular application. The UL-94 vertical test was carried out on samples with 3.2 mm thickness according to ASTM D3801.

Table II. Categorizing the Samples in UL-94V Test Based on ASTM D3801

Condition	V-0	V-1	V-2
After flame time (t_1 or t_2)	≥10 S	≥30 S	≥ 30 S
($t_2 + t_3$) for each specimen	≥ 30S	≥ 60 S	≥ 60 S
Burning the samples to the grip point (with flame or with glowing)	No	No	No
Dripping the samples and make a piece of cotton burning with fire droplets	No	No	Yes

The samples whose burning does not stop are considered as not rated (N.R.).

As mentioned in the standard, the specimen is kept vertical, and then the flame is held under the specimen for 10 s. Taking away the flame, the after-flame time, which is the time span in which the specimen is burning after moving away the flame, is measured. This action is repeated three times, measuring after-flame times (t_1 and t_2) and after-glow time (t_3). Then the flame resistance of the samples is categorized as V-0, V-1, and V-2, as mentioned in the standard, based on the amount of measured after-flame times, which is summarized below in Table II.

Thermal Properties. Oxidative induction time (OIT) of the samples was measured according to ASTM D3895 by differential scanning calorimeter (DSC), DSC 200F3 Maia model, NETZSCH Co, Germany. OIT represents the resistance of the specimen to the oxidation, which can be determined by measuring the time in which the exothermic oxidation commences in a definite temperature when the specimen is heated exposed to the oxygen. For this test, the specimen was placed in DSC and was heated to 200°C with heat flow rate of 10°C/min under the nitrogen flux. Then the temperature was kept at 200°C and the specimen is exposed to the oxygen to observe the oxidative reaction. To determine the relative thermal stability of the specimens and study the decomposition of nanocomposites in the air, thermogravimetric analysis (TGA) and differential thermal analysis (DTA), which is the derivative form of TGA curve, were applied. The test was carried out in the air at the heating rate of 10°C/min using a Shimadzu TGA-50H thermogravimetric analyzer, Japan. In each case, 10 mg of each sample was examined under an air flow rate of 100 mL/min in the temperature range of the ambient temperature to 600°C.

Morphological Properties. The X-ray diffraction (XRD) test is a technique to determine the phase structures and composition of a material. This method is very useful in determining the structure between nanolayers in the nanocomposites. In X-ray method, parallel radiations of X-ray with the same energy are irradiated to the specimens, considering the fact that the irradiated X-ray wave length is an order of distance between atoms of the material. Here, the wave length is an order of the distance between the silicate nanolayers. The samples used for the XRD test were films with dimensions of 3 × 3 mm^2, which were produced by hot press technique. The XRD patterns of the samples were recorded with a Bruker D8 Advance X-ray diffractometer, Germany (using Cu Kα 1.54 Å radiation). The diffraction patterns were collected with a 0.04° 2θ step size and a 2 s count time from 1.4 to 10°. In this range, matrix shows no peak, while nanosilicate shows one peak. The results were applied to investigate the type of placement of nanolayers and their exfoliation in the matrix. The dispersion of MH particles in the matrix was analyzed by scanning electron microscopy (XLC, Philips, UK). The sheets were cryogenically fractured in liquid nitrogen. The fractured surfaces were sputtered with gold before viewing.

RESULTS AND DISCUSSION

Mechanical Properties

Tensile strength and strain at break of the samples obtained from the tensile test are summarized in Table III. In general, incorporation of 55 to 60 wt % of MH is common in fire resistant, halogen-free composite applicable in cable industry. Therefore, the composites of EVA/LDPE/55 wt % MH and EVA/LDPE/60 wt % MH ($VE_{2\text{-}0A0B\text{-}55}$ and $VE_{3\text{-}0A0B\text{-}60}$) were considered as the references. The mechanical properties requirement for developing thin walled, halogen-free, fire-resistant, and low-smoking cable-sheathing compound intended for low voltage application (up to 3–4 kV) have been specified as: tensile strength ≥8 MPa, elongation at break ≥125%, and LOI% >30.[9] According to these criteria, between nanocomposite samples (Tables III and IV) only $V_{\text{-}0A2B\text{-}53}$, VE1 series, $VE_{2\text{-}5A0B\text{-}50}$, and $VE_{3\text{-}0A0B\text{-}60}$ have the required properties. In all the series 1, 2, and 3, it is clear that by replacing some of the MH with OMMT according to Table III, tensile strength increases. This improvement can be attributed to the reinforcing effect of the nanoclay platelets.[3] However, by increment of (MH + OMMTs) from 55 wt % to 60 wt %, it is clear that the tensile strength and also elongation at break show reduction, as it can be seen from the Table III. This is possibly owing to occasional

Table III. Tensile Strength and Elongation at Break of the Composite Specimens

Sample	Tensile strength (MPa)	Elongation at break (%)
VE	17.56 ± 1.5	796.4 ± 20
$V_{\text{-}0A2B\text{-}53}$	11.35 ± 0.5	404.7 ± 36
$V_{\text{-}0A2B\text{-}0}$	19.61 ± 0.8	1126.3 ± 33
$VE_{1\text{-}2A0B\text{-}53}$	9.29 ± 0.7	235.0 ± 48
$VE_{1\text{-}1A1B\text{-}53}$	9.79 ± 1.1	155.0 ± 21
$VE_{1\text{-}0A2B\text{-}53}$	10.68 ± 0.5	132.0 ± 13
$VE_{2\text{-}0A0B\text{-}55}$	8.46 ± 0.5	408.2 ± 35
$VE_{2\text{-}5A0B\text{-}50}$	9.30 ± 0.6	130.0 ± 22
$VE_{2\text{-}2.5A2.5B\text{-}50}$	10.83 ± 0.9	104.7 ± 12
$VE_{2\text{-}0A5B\text{-}50}$	11.13 ± 1	83.3 ± 6
$VE_{3\text{-}0A0B\text{-}60}$	8.12 ± 0.6	310.6 ± 10
$VE_{3\text{-}5A0B\text{-}55}$	8.93 ± 0.5	51.5 ± 3.5
$VE_{3\text{-}2.5A2.5B\text{-}55}$	10.58 ± 1.2	39.5 ± 5
$VE_{3\text{-}2A3B\text{-}55}$	10.75 ± 0.75	45.3 ± 4.5
$VE_{3\text{-}0A5B\text{-}55}$	11.10 ± 0.9	43.0 ± 4

Table IV. Flame Properties of Samples Obtained Based on LOI and UL-94V Tests

Sample	LOI (%)	UL-94V (3.2 mm)
EVA/PE	17 ± 1	N.R.
$V_{-0A2B-53}$	39.5 ± 2.5	V-0
$V_{-0A2B-0}$	17.5 ± 2	N.R.
$VE_{1-2A0B-53}$	35 ± 3	V-0
$VE_{1-1A1B-53}$	35.5 ± 3.2	V-0
$VE_{1-0A2B-53}$	35.5 ± 4	V-0
$VE_{2-0A0B-55}$	29.5 ± 2.5	N.R.
$VE_{2-5A0B-50}$	34 ± 3	N.R.
$VE_{2-2.5A2.5B-50}$	34.5 ± 1.6	N.R.
$VE_{2-0A5B-50}$	35 ± 2.4	N.R.
$VE_{3-0A0B-60}$	31 ± 3	N.R.
$VE_{3-5A0B-55}$	36.5 ± 3.3	V-1
$VE_{3-2.5A2.5B-55}$	36.5 ± 1.3	V-1
$VE_{3-2A3B-55}$	36.5 ± 2.8	V-1
$VE_{3-0A5B-55}$	37 ± 2.2	V-1

N.R.: not rated.

agglomeration of the nanoclays and MH particles in the polymer matrix. It is also conspicuous from Table III that by changing Cloisite 15A with Cloisite 30B, the tensile strength shows more enhancement, as it was seen from the Table III. This could be due to polar structure of Cloisite 30B nanolayers, which causes more attraction between nanoclays and the EVA matrix. Peeterbroeck et al.[10] also stated that hydrogen type attraction is formed between hydroxyl groups of ammonium in Cloisite 30B and acetate groups in EVA, which enhance the tensile strength and therefore reduction in elongation at break.

Flame Properties

The LOI and UL-94 tests are widely used to evaluate fire retardancy (FR) properties of materials and to display FR formulations.[11,12] Table IV lists the LOI and UL-94 results obtained for the different formulations of EVA/LDPE/MH/OMMTs composites in Table I. It can be seen from the table that the LOI values of the reference samples containing 55 wt % and 60 wt % of MH ($VE_{2-0A0B-55}$ and $VE_{3-0A0B-60}$) increased rapidly to around 30, comparing with LOI of EVA/LDPE sample without any OMMTS, which was 17. MH acts in both the condensed and gaseous phases. It is decomposed via an endothermic reaction and reduces the temperature of the burning material with releasing water into the gas phase, which dilutes the flame.[13] As another mechanism to retard the flammability of the polymer, MH also plays a role as a catalyst for the oxidation of the carbonaceous remains, decreasing the CO/CO_2 part.[5] The oxides like CO_2, formed by the decomposition, can help the formation of an insulative charred layer which could act as a shield for the polymer against the flame. Additionally, the decomposed product (MgO) could insulate the substrate from the heat source by enhancement of the char formation. These char-like products produced via thermal dehydration of polymer chains, which is called as the "β-elimination reaction" in the texts, are able to insulate the substrate from the oxygen and the heat source, and also cut down the amount of carbon entering the flame, and therefore could majorly function in the flame retardancy and suppression of produced smoke.[14] The substitution of MH by 2 or 5 wt % of OMMT, leads to improvement of LOI and UL-94V results, as it is shown in Table IV. It can be considered that OMMTs could significantly reinforce the protective residual formed by MH against the flame, and therefore help to achieve higher flame resistant polymer.[15] Comparing VE_1 and VE_2 series, the reduction of LOI by increasing the amount of OMMT can be seen, while keeping a constant amount of total fillers (55 wt %), which is maybe due to the MH reduction as the main flame retardant. Moreover, as the amount of OMMT is enhanced, the nanolayers might agglomerate in the bulk of polymer matrix, and dispersion of OMMTs in a nanoscale is weakened which could reduce the LOI value.[6] In all of the series, by changing the type of nanoparticles from C15A to C30B, LOI does not change considerably, however, LOI values of the samples containing C30B is a little more than that of the samples containing C15A. According to TG/DTA data sheet of these nanoparticles, this may be because of more char formation of C30B, and therefore higher fire protection of samples with C30B.

Comparing the LOI values of the two samples of $VE_{1-0A2B-53}$ and $V_{-0A2B-53}$, LOI changes about 11% in spite of containing equal content of MH and C30B fillers. This is as a consequence of more acetic acid produced by $V_{-0A2B-53}$ sample while burning that could cause acceleration of water release by MH and more resistant toward the flame, and therefore higher amount of

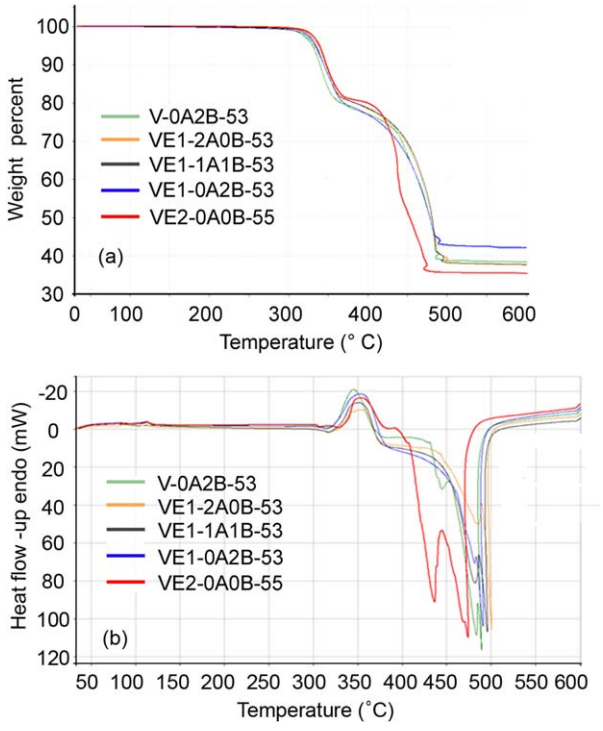

Figure 1. a) TGA and b) DTA diagrams of $V_{-0A2B-53}$, $VE_{1-2A0B-53}$, $VE_{1-1A1B-53}$, $VE_{1-0A2B-53}$, and $VE_{2-0A0B-55}$ samples. [Color figure can be viewed in the online issue, which is available at wileyonlinelibrary.com.]

Table V. TGA results of $VE_{2\text{-}0A0B\text{-}55}$, $V_{\text{-}0A2B\text{-}53}$, $VE_{1\text{-}2A0B\text{-}53}$, $VE_{1\text{-}1A1B\text{-}53}$, and $VE_{1\text{-}0A2B\text{-}53}$ Samples

Samples	$T_{p,1}$ (°C)	$T_{p,2}$ (°C)	Char (%)
$VE_{2\text{-}0A0B\text{-}55}$	346.14	435.59	35.739 ± 0.8
$V_{\text{-}0A2B\text{-}53}$	342.07	480.58	38.907 ± 0.65
$VE_{1\text{-}2A0B\text{-}53}$	346.01	481.34	38.014 ± 0.5
$VE_{1\text{-}1A1B\text{-}53}$	347.04	478.92	38.222 ± 1.2
$VE_{1\text{-}0A2B\text{-}53}$	351.96	479.13	42.701 ± 0.9

LOI.[12,16] LOI of $V_{\text{-}0A2B\text{-}0}$ sample is approximately equal to LOI of $V_{\text{-}0A2B\text{-}53}$ sample. This implies that without traditional flame retardant, the nanocomposite alone is not a solution to prevention of flammability. However, due to its synergistic effect in flame retardancy with traditional flame retardant materials, nanoclays can be used in combination with those conventional substances. In such systems, the nanosilicate particles maintain mechanical properties of the polymer which already have been weakened in presence of high amount of MH.[12,16] Based on LOI test, it is believed that inadequate layered nanoclays in the nanocomposite can not form a rigid insulation layer on the burning surface, and it may flow away with dripping molten flaming materials. Therefore, the addition of organoclay at a low level is insufficient to provide effective flame retardancy.[17] If the char formation can increase, the same flame retardancy can be achieved using the lower filling ratio of fillers. In this way, the lower filling ratio causes the lower density of compound and higher production speed without compromising the surface smoothness of the resultant products.[18] As it can be seen in Table IV, by addition of 55% MH in the $VE_{2\text{-}0A0B\text{-}55}$ sample, dripping in the burning test was not stopped; however, by addition of the nanoclay, dripping completely was stopped. This could be attributed to the fact that when the nanoclay is added into the EVA/LDPE polymer matrix, the viscosity of the composite increases, which prevents the dripping of the nanocomposite sample while burning.[6] According to Table IV, addition of only 2% OMMT is sufficient to obtain V-0 rating and surprisingly more content of OMMT leads to weaker results. As discussed for LOI test results, this might be due to agglomeration of the nanolayers in the polymer matrices.[6]

Thermal Properties

Thermogravimetric analysis (TGA) is widely used to characterize the thermal stability of polymers. The mass loss of the polymer due to the volatilization of products generated by thermal decomposition is monitored as a function of temperature. The experimental conditions of the degradation highly influence the reaction mechanism of the degradation course. EVA is recognized to decompose in two consecutive steps. The first step is identical in both oxidative and nonoxidative conditions. It happens between 350°C and 400°C, which is related to the loss of acetic acid. The second step includes the thermal decomposition of the obtained unsaturated backbone either by more radical scissions (nonoxidative decomposition), or by thermal combustion (oxidative decomposition).[6] According to the researchers in this area, under nonoxidative decomposition, the EVA nanocomposite shows smaller reduction in thermal stability compared to that of pure EVA. On the contrary, when it decomposes in the air, the same nanocomposite exhibits a rather large increase in the thermal stability. The maximum of the second and first decomposition peak is shifted about 40°C to the higher temperatures and remains unchanged respectively.[16,19] In this work, the TGA test was carried out under air flow. Figure 1(a,b) are TGA and DTA curves of the composite samples, respectively. Some of the information from these curves have been brought in Tables V and VI. In Table V, $T_{p,1}$ and $T_{p,2}$ represent the temperatures that maximum mass loss rate occurs in the first and second decomposition steps, respectively. By addition of OMMT, $T_{p,1}$ does not change considerably, but $T_{p,2}$ increases about 45°C.

The mass losses in the primary sections of the curves are attributed to the combinational release of acetic acid from the EVA, water from decomposition of the $Mg(OH)_2$, and organic

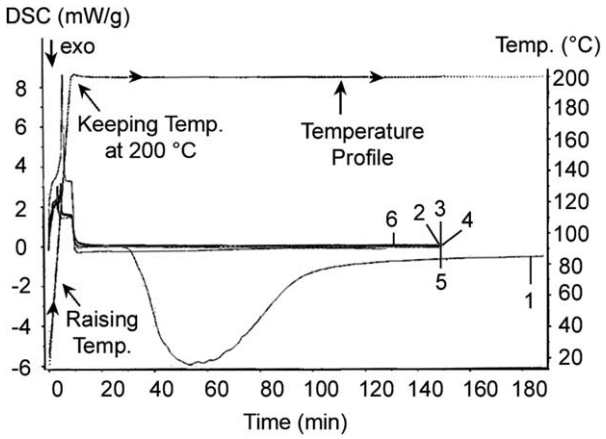

Figure 2. OIT diagram of selected samples: (1) $VE_{2\text{-}0A0B\text{-}55}$, (2) $V_{-0A2B\text{-}53}$, (3) $VE_{1-2A0B\text{-}53}$, (4) $VE_{1\text{-}1A1B\text{-}53}$, (5) $VE_{1\text{-}0A2B\text{-}53}$, (6) $VE_{2-5A0B\text{-}50}$.

Table VI. DTA Results of the $VE_{2\text{-}0A0B\text{-}55}$, $V_{-0A2B\text{-}53}$, $VE_{1\text{-}2A0B\text{-}53}$, $VE_{1\text{-}1A1B\text{-}53}$ and $VE_{1\text{-}0A2B\text{-}53}$ Samples

	First step				Second step			
Sample	T_i (°C)	T_f (°C)	T_p (°C)	ΔH (J/g)	T_i (°C)	T_f (°C)	T_p (°C)	ΔH (J/g)
$VE_{2\text{-}0A0B\text{-}55}$	330	386.96	354.74	340.35	391.59	491.62	436.38	−3553.38
$V_{\text{-}0A2B\text{-}53}$	320	378.52	345.59	412.96	424.36	504.45	489.35	−1953.45
$VE_{1\text{-}2A0B\text{-}53}$	315	381.41	355.59	381.15	423.71	513.26	500.55	−1766.16
$VE_{1\text{-}1A1B\text{-}53}$	316	384.95	353.80	394.89	402.45	514.01	495.68	−1675.11
$VE_{1\text{-}0A2B\text{-}53}$	313	397.37	355.29	525.01	398.29	514.21	490.76	−1496.88

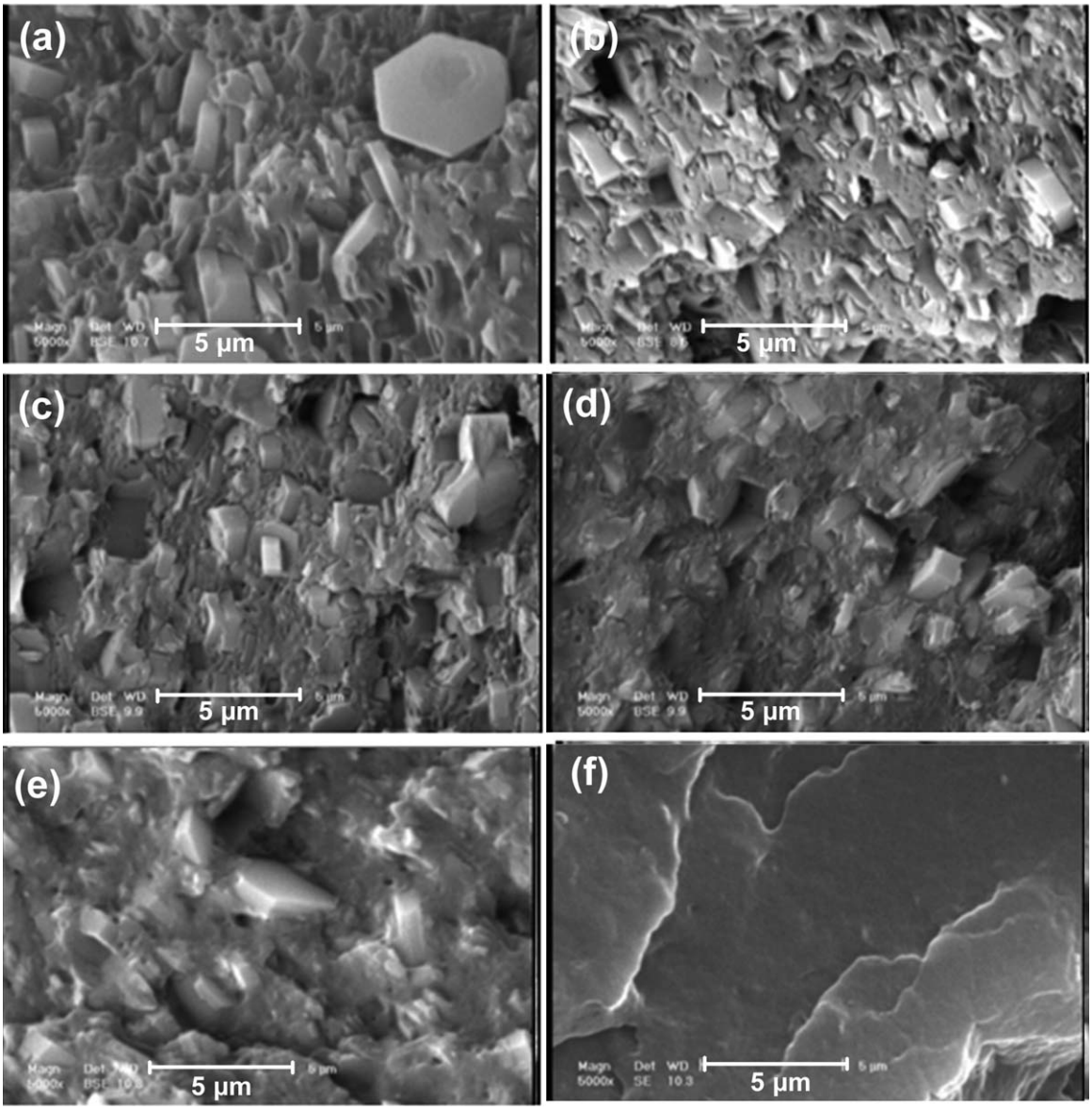

Figure 3. SEM micrographs of tensile fracture surfaces of: (a) $VE_{2\text{-}0A0B\text{-}55}$, (b) $VE_{1\text{–}2A0B\text{-}53}$, (c) $VE_{1\text{-}1A1B\text{-}53}$, (d) $VE_{1\text{-}0A2B\text{-}53}$, (e) $V_{-0A2B\text{-}53}$, (f) $V_{-0A2B\text{-}0}$ nanocomposites (magnification ×5000).

coating from the nanomaterials. These results suggest that the montmorillonite accelerates the rate of acetic acid loss from EVA, and/or accelerate the rate of dehydration of $Mg(OH)_2$.[20] According to Figure 1(a), the presence of OMMT in the nanocomposites causes the beginning of mass loss slightly shifted to lower temperatures compared with that of the sample without OMMT ($VE_{2\text{-}0A0B\text{-}55}$). This is due to the decomposition of the organic section of OMMT, which starts around 200°C.[21] As the polymer nanocomposite is heated, this organic part begins to degrade first, forming acidic sites on the surface of montmorillonite. As the EVA decomposes with the release of acetate groups to form poly(vinyl alcohol)-like structure, the acidic sites on the clay surface catalyze cross-linking and aromatization reactions, resulting in carbon char formation, which plays an important role on deterring the combustion.[22] Such information indicates that postpone of thermal degradation is mainly due to a reduction in the rate of development of the volatile products. The origin of a shift in mass loss by addition of nanoparticles to EVA matrix was studied by Zanetti et al.[23] The important postpone in weight loss of EVA nanocomposites when exposed to air has been attributed to the barrier effect developed by the presence of dispersed nanoclay platelets, whose exfoliated structures deteriorate upon matrix degradation, which forms an insulation layer. Actually, such morphology development provokes a reduction in both of the volatile thermo-oxidation products spreading out and also oxygen diffusion from the gas phase into the polymer matrix.[10,17] Montmorillonite nanolayers consist of tetrahedral-octahedral silicate plates with well-ordered spatial structural design. Therefore, when exfoliated within a polymeric matrix, silicate nanolayers are expected to hinder thermal degradation due to the lower heat diffusion toward the polymeric molecules. It can therefore be

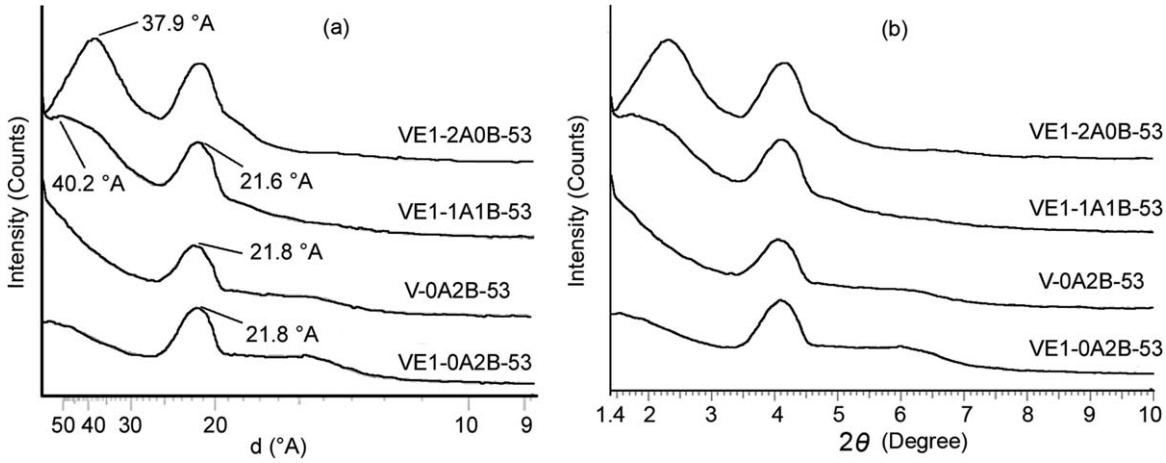

Figure 4. XRD diagram of $VE_{1–2A0B-53}$, $VE_{1-1A1B-53}$, $V_{–0A2B-53}$, and $VE_{1-0A2B-53}$ samples.

concluded that thermal degradation of the aliphatic chains in the EVA/LDPE matrix can be retarded by an improvement in the exfoliation of the silicate layers which works as a barrier for heat diffusion, most probably due to a Labyrinth effect.[24] The residual layer insulates the underlying materials and slows down the release of the volatile products produced throughout the decomposition.[25] It should come to consideration that the more residual weight left after combustion is attributed the better flame retardancy properties, implying less release of volatile produced products while burning. TGA diagram shows that the residual of C30B contained sample (i.e. $VE_{1-0A2B-53}$) is more than that of C15A contained specimen (i.e. $VE_{1-2A0B-53}$), and also had higher amount of LOI value. Less residual of $V_{-0A2B-53}$ with respect to $VE_{1-0A2B-53}$ is attributed to the more EVA content and thus more release of acetic acid. The DTA data of the samples obtained from DTA diagram in Figure 1(b) are tabulated in Table VI.

As it can be seen in DTA results, heat absorption, ΔH, in first and second steps of degradation increases and decreases, respectively. This indicates improvement of flame retardancy. In this point of view, C30B is better than C15A that could be due to its more char formation. Figure 2 shows Oxidative Induction Time (OIT) diagram of selected samples. OIT of $VE_{2-0A0B-55}$ is about 20 min, however, the OIT increases to more than 120 min in presence of OMMT for all of the EVA nanocomposite samples used. The reason for this, as discussed about TGA/DTA, is increasing the char formation that is produced under oxidative condition and in presence of nanoparticles.

Morphological Studies

SEM was used to observe dispersion of the filler particles in the polymer matrix. Images of fractured surfaces of the samples with 5000× magnification are shown in Figure 3(a–f). According to the SEM micrograph of nanocomposites, the MH particles are platy clear in the structures and have a moderately broad particle size distribution and uniform dispersion. The poor adhesion between the MH particles and EVA/LDPE matrix is observed in the sample without the nanoclay, $VE_{2-0A0B-55}$, as shown in Figure 3(a). According to the Figure 3(b–d), the MH particles wetting was improved with increasing of C30B nanoparticle part in the nanocomposite samples, in comparison with the SEM of nanocomposites containing dominant amount of C15A nanoclays. In the nanocomposite containing only EVA matrix and 2 wt % C30B nanoparticles ($V_{-0A2B-53}$) based on Figure 3(e), the MH particles were well wetted by EVA that may lead to a good adhesion between MH particles and the EVA matrix. Figure 3(f) shows the SEM micrograph of the EVA matrix nano-composite with 2 wt % C30B nanoclay and without MH ($V_{-0A2B-0}$), whose fracture surface indicates a laminar morphology. X-ray diffraction (XRD) analysis is used to measure the dispersion of nanoparticle layers. In this study, the particles are organo-modified nanoclays. In intercalated nanocomposites, the diffusion of the polymer chains between nanoclay layers usually increases the interlayer spacing, comparing with the spacing of the organo-clay itself, leading to a shift of the diffraction peak toward lower angle values.[26] The initial distance between nanolayers before incorporation with the polymer matrix, or known as d-spacing (d_{001}), in Cloisite 15A and Cloisite 30B are 31.5°A and 18.5°A, respectively. After mixing of the nanoparticles (C15A and C30B) with the polymer matrix, shifting of d_{001} to the higher interlayer distances supports the semi exfoliation/exfoliation of nanolayers in the composite samples. The peak shifting indicates an intercalation structure of nanoparticles or placement of polymer chains between the silicate layers in the nanocomposite samples, enhancing the interlayer spacing. Figure 4(a,b) shows the XRD diagrams of $VE_{1-2A0B-53}$, $VE_{1-1A1B-53}$, $V_{-0A2B-53}$, and $VE_{1-0A2B-53}$ samples based on d-spacing and 2θ, respectively. The XRD pattern of the $VE_{1-2A0B-53}$ sample presents two peaks, around 37.9°A and 22°A, respectively. The latter peak is probably due to the part of Cloisite 15A nanoparticles that were not modified by quaternary ammonium salt, or could be due to the thermal degradation of alkyl ammonium groups in Cloisite 30B nanoparticles via sample preparation process.[27–32] As it can be seen from the pattern in Figure 4(a), d-spacing of clay nanoparticles in $VE_{1-2A0B-53}$ sample is 37.9°A which had an enhancement of 6.4°A in de-spacing comparing with that of original C15A nanoclay(≈20%). This increment implies a good combination of C15A

nanoparticles with the EVA/LDPE matrix. In both of XRD patterns of $V_{-0A2B-53}$, and $VE_{1-0A2B-53}$ samples (both including 2 wt % of C30B nanoclays), d-sapacing turned out to be 21.8°A, which enhanced 3.3°A (≈17.8 %) comparing with d_{001} of C30B nanoclay layers. Widened XRD peak related to C30B nanoclayes which supports the existence of exfoliated structure of nanolayers in the bulk of polymer matrix.[7] In $VE_{1-1A1B-53}$, d-spacing related to C30B nanoclay obtained 21.6°A, which was enhanced about 3.1°A (≈16.7%). In addition, de-spacing of C15A nanoparticles in this specimen was 40.2°A showing the increment of 8.7°A (≈28%) in basal spacing. The XRD pattern of the $VE_{1-1A1B-53}$ sample exhibits a scattered peak for C15A nanoclay toward longer d-spacing (lower angles) as it conspicuous from Figure 4(a,b). This could also be related to the development of nanoclay exfoliated structure.[7] Such a high increase in interlayer spacing indicates a better affinity of the polymer matrix with the C15A[10] and a better dispersion of clay aggregates.[27] The compatibility of C15A with EVA/LDPE matrix is also more than C30B, mainly due to its more gallery distance which makes it easier for polymer chains to diffuse between nanolayers. Parenthetically, to make a good attraction between nanoparticles and polymer matrix, polar structure of C30B supports the enhancement of attraction due forming hydrogen bond between hydroxyl groups of C30B nanoclays and acetate groups of EVA matrix, helping the intercalation or even exfoliation of C30B nanoparticles in the nanocomposites.

CONCLUSION

According to the limiting oxygen index (LOI) data and UL-94V test, the addition of MH and OMMT to the EVA/LLDPE exhibits a synergistic effect on the flame retardancy. In all samples with replacement of MH by OMMT, the LOI values were increased. The addition of 2 wt % OMMT to EVA/LDPE/MH composites was sufficient to achieve a significant improvement in thermal stability and flame retardancy, while keeping mechanical properties. Also, addition of more OMMT not only did not improve flame properties, but also resulted in deterioration of mechanical properties. The morphology studies show a good compatibility of Cloisite 15A with EVA/LDPE matrix.

REFERENCES

1. Zhang, L.; Li, C. Z.; Zhou, Q.; Shao, W. *J. Mater. Sci.* **2007**, *42*, 4227.
2. Basfar, A. A. *Radiat. Phys. Chem.* **2002**, *63*, 505.
3. Haurie, L.; Fernandez, A. I.; Velasco, J. I.; Chimenos, J. M.; Cuesta, J. M. L.; Espiell, F. *Polym. Degrad. Stabil.* **2007**, *92*, 1082.
4. Haurie, L.; Fernandez, A.; Velasco, J.; Chimenos, J. M.; Cuesta, J. M. L.; Espiell, F. *Polym. Degrad. Stab.* **2006**, *91*, 989.
5. Camino, G.; Maffezzoli, A.; Bragliac, M.; De Lazzaro, M.; Zammarano, M. *Polym. Degrad. Stab.* **2001**, *74*, 457.
6. Zhang, Y.; Hu, Y.; Song, L.; Wu, J.; Fang, S. *Polym. Adv. Technol.* **2008**, *19*, 960.
7. Szep, A.; Szabo, A.; Toth, N.; Anna, P.; Marosi, G. *Polym. Degrad. Stab.* **2006**, *91*, 593.
8. Yang, X.; Li, Q.; Chen, Z.; Han, H.; Jing, H. *J. Compos. Mater.* **2009**, *43*, 2785.
9. Naskar, K.; Mohanty, S.; Nando, G. B. *J. Appl. Polym. Sci.* **2007**, *104*, 2839.
10. Peeterbroeck, S.; Alexandre, M.; Jerome, R.; Dobois, P. *Polym. Degrad. Stab.* **2005**, *90*, 288.
11. Fu, M.; Qu, B. *Polym. Degrad. Stab.* **2004**, *85*, 633.
12. Bras, M. L.; Wilkie, C. A.; Bourbigot, S.; Duquesne, S.; Jama, C. Fire Retardancy of Polymers, New Applications of Mineral Fillers; Royal Society of Chemistry: Cambridge, **2005**.
13. Du, L.; Qu, B.; Xu, Z. *Polym. Degrad. Stab.* **2006**, *91*, 995.
14. Yeh, J. T.; Yang, M. J.; Hsieh, S. H. *Polym. Degrad. Stab.* **1998**, *61*, 465.
15. Laoutid, F.; Gaudon, P.; Taulemesse, J. M.; Lopez Cuesta, J. M.; Velasco, J. I.; Piechaczyk, A. *Polym. Degrad. Stab.* **2006**, *91*, 3074.
16. Beyer, G. *J. Fire. Sci.* **2005**, *23*, 75.
17. Chuang, T. H.; Guo, W.; Cheng, K. C.; Chen, S. W.; Wang, H. T.; Yen, Y. Y. *J. Polym. Res.* **2004**, *11*, 169.
18. Sener, A. A.; Demirhan, E. *Mater. Design.* **2008**, *29*, 1376.
19. Cardenas, M. A.; Garcia-Lopez, D.; Gobernado-Mitre, I.; Merino, J. M.; Pastor, J. M.; Martinez, J. D. D.; Barbeta, J.; Calveras, D. *Polym. Degrad. Stab.* **2008**, *93*, 2032.
20. Cogen, J. M.; Lin, T. S.; Morgan, A. B. Garcés, J. M. Novel Synthetic Nanocomposite Materials and Their Application in Polyolefin-Based Wire and Cable Compounds. In: *Proceedings of the 52nd International Wire and Cable Symposium.* The Dow Chemical Company, LOES Form Number 311, **2003**.
21. Clerc, L.; Ferry, L.; Leory, E.; Lopez-Cuesta, J. M. *Polym. Degrad. Stab.* **2005**, *88*, 504.
22. Morgan, A. B. *Polym. Degrad. Stab.*, **2006**, *17*, 206.
23. Zanetti, M.; Camino, G.; Thomann, R.; Mülhaupt, R. *Polymer* **2001**, *42*, 4501.
24. Valera-Zaragoza, M.; Ramirez-Vargas, E.; Medellın-Rodrıguez, F. J.; Huerta-Martınez, B. M. *Polym. Degrad. Stab.* **2006**, *91*, 1319.
25. Zhang, X.; Gue, F.; Chen, J.; Wang, G.; Liu, H. *Polym. Degrad. Stab.* **2005**, *87*, 411.
26. Alexandre, M.; Dubois, P. *Mater. Sci. Eng.* **2000**, *28*, 1.
27. Lee, K. M.; Han, C. D. *Macromolecules* **2003**, *36*, 7165.
28. Calcagno, C. I. W.; Mariani, C. M.; Teixeira, S. R.; Mauler, R. S. *Compos. Sci. Technol.* **2008**, *68*, 2193.
29. Kim, N. H.; Malhotra, S. V.; Xanthos, M. *Microporous Mesoporous Mater.* **2006**, *96*, 29.
30. Torre, L.; Lelli, G.; Kenny, J. M. *J. Appl. Polym. Sci.* **2006**, *100*, 4957.
31. Nazockdast, E.; Nazockdast, H.; Goharpey, F. *Polym. Eng. Sci.* **2008**, *48*, 1240.
32. Dennis, H.R.; Hunter, D.L.; Chang, D.; Kim, S.; White, J. L.; Cho, J. W.; Paul, D. R. *Polymer* **2001**, *42*, 9513.